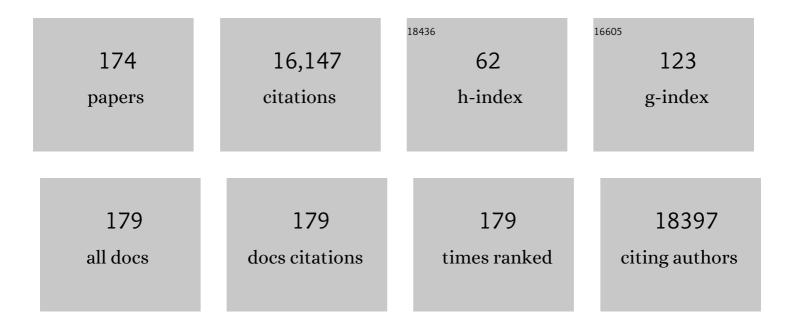
## Zhao-Xiong Xie

List of Publications by Year in descending order

Source: https://exaly.com/author-pdf/4419031/publications.pdf Version: 2024-02-01



#	Article	IF	CITATIONS
1	Platinumâ€Tin/Tin Oxide/CNT Catalysts for Highâ€Performance Electrocatalytic Ethanol Oxidation. Chemistry - A European Journal, 2022, 28, .	1.7	4
2	Introducing oxophilic metal and interstitial hydrogen into the Pd lattice to boost electrochemical performance for alkaline ethanol oxidation. Journal of Materials Chemistry A, 2022, 10, 1735-1741.	5.2	35
3	Pt Particle Size Affects Both the Charge Separation and Water Reduction Efficiencies of CdS–Pt Nanorod Photocatalysts for Light Driven H <sub>2</sub> Generation. Journal of the American Chemical Society, 2022, 144, 2705-2715.	6.6	80
4	Co3O4 nanocrystals as matrices for the detection of amino acids, harmful additives and pesticide residues by MALDI-TOF MS. Talanta, 2022, 242, 123299.	2.9	8
5	Singleâ€Atom Molybdenum Engineered Platinum Nanocatalyst for Boosted Alkaline Hydrogen Oxidation. Advanced Energy Materials, 2022, 12, .	10.2	53
6	Hot-electron-induced CO2 hydrogenation on Au@AuRu/g-C3N4 plasmonic bimetal–semiconductor heterostructure. Chemical Engineering Journal, 2022, 443, 136482.	6.6	13
7	Equilibrated PtIr/IrO <i><sub>x</sub></i> Atomic Heterojunctions on Ultrafine 1D Nanowires Enable Superior Dualâ€Electrocatalysis for Overall Water Splitting. Small, 2022, 18, e2201333.	5.2	21
8	Two-Dimensionally Assembled Pd–Pt–Ir Supernanosheets with Subnanometer Interlayer Spacings toward High-Efficiency and Durable Water Splitting. ACS Catalysis, 2022, 12, 5305-5315.	5.5	26
9	Rational design of two-dimensional flaky Fe/void/C composites for enhanced microwave absorption properties. Dalton Transactions, 2022, 51, 8705-8713.	1.6	9
10	Oxidative Stability Matters: A Case Study of Palladium Hydride Nanosheets for Alkaline Fuel Cells. Journal of the American Chemical Society, 2022, 144, 8106-8114.	6.6	27
11	Ultrafast Anisotropic Evolution of Photoconductivity in Sb <sub>2</sub> Se <sub>3</sub> Single Crystals. Journal of Physical Chemistry Letters, 2022, 13, 4988-4994.	2.1	7
12	Tailoring the Chemical Potential of Crystal Growth Units to Tune the Bulk Structure of Nanocrystals. Small Methods, 2021, 5, e2000447.	4.6	6
13	Synthesis of hollow rod-like hierarchical structures assembled by CoFe/C nanosheets for enhanced microwave absorption. Journal of Materials Chemistry C, 2021, 9, 13860-13868.	2.7	21
14	Concave nano-octahedral alloys: wet chemical synthesis of bimetallic Pt–Pd nanocrystals with high-index {hhl} Facets. Dalton Transactions, 2021, 50, 12083-12087.	1.6	6
15	Plasmonic nanoreactors regulating selective oxidation by energetic electrons and nanoconfined thermal fields. Science Advances, 2021, 7, .	4.7	43
16	Amplified Interfacial Effect in an Atomically Dispersed RuO <sub>x</sub> â€onâ€Pd 2D Inverse Nanocatalyst for Highâ€Performance Oxygen Reduction. Angewandte Chemie, 2021, 133, 16229-16236.	1.6	12
17	Amplified Interfacial Effect in an Atomically Dispersed RuO <sub>x</sub> â€onâ€Pd 2D Inverse Nanocatalyst for Highâ€Performance Oxygen Reduction. Angewandte Chemie - International Edition, 2021, 60, 16093-16100.	7.2	49
18	Atomically dispersed Pt/CeO2 catalyst with superior CO selectivity in reverse water gas shift reaction. Applied Catalysis B: Environmental, 2021, 291, 120101.	10.8	75

#	Article	IF	CITATIONS
19	Heterogeneous <i>fcc</i> -Pt/ <i>hcp</i> -PtBi Thick-Edge Nanoplates with Enhanced Activity for Formic Acid Oxidation. ACS Applied Energy Materials, 2021, 4, 9190-9197.	2.5	15
20	Trimetallic PtNiCo branched nanocages as efficient and durable bifunctional electrocatalysts towards oxygen reduction and methanol oxidation reactions. Journal of Materials Chemistry A, 2021, 9, 23444-23450.	5.2	49
21	Effect of Rutile Content on the Catalytic Performance of Ru/TiO <sub>2</sub> Catalyst for Low-Temperature CO <sub>2</sub> Methanation. ACS Sustainable Chemistry and Engineering, 2021, 9, 14288-14296.	3.2	34
22	Dynamic Phase Transition of Iron Oxycarbide Facilitated by Pt Nanoparticles for Promoting the Reverse Water Gas Shift Reaction. ACS Catalysis, 2021, 11, 14586-14595.	5.5	10
23	Highly efficient ethylene production via electrocatalytic hydrogenation of acetylene under mild conditions. Nature Communications, 2021, 12, 7072.	5.8	51
24	Synthesis of PdH0.43 nanocrystals with different surface structures and their catalytic activities towards formic acid electro-oxidation. Science China Materials, 2020, 63, 375-382.	3.5	19
25	Surface structure-dependent electrocatalytic reduction of CO <sub>2</sub> to C1 products on SnO <sub>2</sub> catalysts. Sustainable Energy and Fuels, 2020, 4, 600-606.	2.5	5
26	Synthesis of sandwich-like Co <sub>15</sub> Fe <sub>85</sub> @C/RGO multicomponent composites with tunable electromagnetic parameters and microwave absorption performance. Nanoscale, 2020, 12, 18790-18799.	2.8	39
27	Biomimetic Metal–Organic Framework Composite-Mediated Cascade Catalysis for Synergistic Bacteria Killing. ACS Applied Materials & Interfaces, 2020, 12, 36996-37005.	4.0	78
28	Critical Roles of Doping Cl on Cu <sub>2</sub> O Nanocrystals for Direct Epoxidation of Propylene by Molecular Oxygen. Journal of the American Chemical Society, 2020, 142, 14134-14141.	6.6	51
29	PtCo-excavated rhombic dodecahedral nanocrystals for efficient electrocatalysis. Nanoscale Advances, 2020, 2, 4881-4886.	2.2	9
30	Efficient Hot Electron Transfer from Small Au Nanoparticles. Nano Letters, 2020, 20, 4322-4329.	4.5	92
31	The function of metal–organic frameworks in the application of MOF-based composites. Nanoscale Advances, 2020, 2, 2628-2647.	2.2	136
32	Edge Enrichment of Ultrathin 2D PdPtCu Trimetallic Nanostructures Effectuates Top-Ranked Ethanol Electrooxidation. Nano Letters, 2020, 20, 5458-5464.	4.5	90
33	<i>In situ</i> construction and post-electrolysis structural study of porous Ni <sub>2</sub> P@C nanosheet arrays for efficient water splitting. Inorganic Chemistry Frontiers, 2020, 7, 2960-2968.	3.0	14
34	A New Catalytic System with Balanced Activity and Durability toward Oxygen Reduction. ChemCatChem, 2020, 12, 4817-4824.	1.8	3
35	Facile synthesis of clean PtAg dendritic nanostructures with enhanced electrochemical properties. Inorganic Chemistry Frontiers, 2020, 7, 1250-1256.	3.0	4
36	Quatermetallic Pt-based ultrathin nanowires intensified by Rh enable highly active and robust electrocatalysts for methanol oxidation. Nano Energy, 2020, 71, 104623.	8.2	64

#	Article	IF	CITATIONS
37	Optimization of gold–palladium core–shell nanowires towards H <sub>2</sub> O <sub>2</sub> reduction by adjusting shell thickness. Nanoscale Advances, 2020, 2, 785-791.	2.2	7
38	Nanosheet-assembled, hollowed-out hierarchical γ-Fe <sub>2</sub> O <sub>3</sub> microrods for high-performance gas sensing. Journal of Materials Chemistry A, 2020, 8, 3754-3762.	5.2	43
39	Atomically dispersed hierarchically ordered porous Fe–N–C electrocatalyst for high performance electrocatalytic oxygen reduction in Zn-Air battery. Nano Energy, 2020, 71, 104547.	8.2	206
40	N-doped carbon shell encapsulated PtZn intermetallic nanoparticles as highly efficient catalysts for fuel cells. Nano Research, 2019, 12, 2490-2497.	5.8	54
41	One-step synthesis of thermally stable artificial multienzyme cascade system for efficient enzymatic electrochemical detection. Nano Research, 2019, 12, 3031-3036.	5.8	28
42	Photo-induced Au–Pd alloying at TiO <sub>2</sub> {101} facets enables robust CO <sub>2</sub> photocatalytic reduction into hydrocarbon fuels. Journal of Materials Chemistry A, 2019, 7, 1334-1340.	5.2	89
43	A nano-reactor based on PtNi@metal–organic framework composites loaded with polyoxometalates for hydrogenation–esterification tandem reactions. Nanoscale, 2019, 11, 3292-3299.	2.8	31
44	Efficient oxygen reduction on sandwich-like metal@N–C composites with ultrafine Fe nanoparticles embedded in N-doped carbon nanotubes grafted on graphene sheets. Nanoscale, 2019, 11, 12610-12618.	2.8	26
45	Sierpinski gasket-like Pt–Ag octahedral alloy nanocrystals with enhanced electrocatalytic activity and stability. Nano Energy, 2019, 61, 397-403.	8.2	29
46	Palladium NPs supported on sulfonic acid functionalized metal–organic frameworks as catalysts for biomass cascade reactions. Dalton Transactions, 2019, 48, 5515-5519.	1.6	20
47	Hollow porous rhodium nanoballs. Chemical Communications, 2019, 55, 4989-4992.	2.2	15
48	Excavated RhNi alloy nanobranches enable superior CO-tolerance and CO <sub>2</sub> selectivity at low potentials toward ethanol electro-oxidation. Journal of Materials Chemistry A, 2019, 7, 26266-26271.	5.2	22
49	Excavated Rh nanobranches boost ethanol electro-oxidation. Materials Today Energy, 2019, 11, 120-127.	2.5	22
50	Monocrystalline platinum–nickel branched nanocages with enhanced catalytic performance towards the hydrogen evolution reaction. Nanoscale, 2018, 10, 5072-5077.	2.8	39
51	Chemically initiated liquid-like behavior and fabrication of periodic wavy Cu/CuAu nanocables with enhanced catalytic properties. Nanoscale, 2018, 10, 9012-9020.	2.8	8
52	Preparation of 3D hierarchical porous Co <sub>3</sub> O <sub>4</sub> nanostructures with enhanced performance in lithium-ion batteries. RSC Advances, 2018, 8, 3218-3224.	1.7	12
53	Ultrafine ZnO quantum dot-modified TiO <sub>2</sub> composite photocatalysts: the role of the quantum size effect in heterojunction-enhanced photocatalytic hydrogen evolution. Catalysis Science and Technology, 2018, 8, 1296-1303.	2.1	55
54	Shell-Thickness-Dependent Biexciton Lifetime in Type I and Quasi-Type II CdSe@CdS Core/Shell Quantum Dots. Journal of Physical Chemistry C, 2018, 122, 14091-14098.	1.5	47

#	Article	IF	CITATIONS
55	Synthesis of u-channelled spherical Fe <sub>x</sub> (Co <sub>y</sub> Ni <sub>1â^'y</sub> ) <sub>100â^'x</sub> Janus colloidal particles with excellent electromagnetic wave absorption performance. Nanoscale, 2018, 10, 1930-1938.	2.8	67
56	Stable palladium hydride as a superior anode electrocatalyst for direct formic acid fuel cells. Nano Energy, 2018, 44, 127-134.	8.2	131
57	Solvent-dependent evolution of cyclic penta-twinned rhodium icosahedral nanocrystals and their enhanced catalytic properties. Nano Research, 2018, 11, 656-664.	5.8	19
58	Rationally Armoring PtCu Alloy with Metalâ€Organic Frameworks as Highly Selective Nonenzyme Electrochemical Sensor. Advanced Materials Interfaces, 2018, 5, 1801168.	1.9	19
59	Toward Rationally Designing Surface Structures of Micro- and Nanocrystallites: Role of Supersaturation. Accounts of Chemical Research, 2018, 51, 2880-2887.	7.6	53
60	Surface Engineering Protocol To Obtain an Atomically Dispersed Pt/CeO <sub>2</sub> Catalyst with High Activity and Stability for CO Oxidation. ACS Sustainable Chemistry and Engineering, 2018, 6, 14054-14062.	3.2	102
61	An anionic <i>sod</i> -type terbium-MOF with extra-large cavities for effective anthocyanin extraction and methyl viologen detection. Chemical Communications, 2018, 54, 5972-5975.	2.2	28
62	Origin of symmetry breaking in the seed-mediated growth of bi-metal nano-heterostructures. Science Bulletin, 2018, 63, 892-899.	4.3	10
63	Optimizing the Electromagnetic Wave Absorption Performances of Designed Co <sub>3</sub> Fe <sub>7</sub> @C Yolk–Shell Structures. ACS Applied Materials & Interfaces, 2018, 10, 28839-28849.	4.0	147
64	Real-space imaging with pattern recognition of a ligand-protected Ag374 nanocluster at sub-molecular resolution. Nature Communications, 2018, 9, 2948.	5.8	26
65	Size and Shape Controlled Synthesis of Pd Nanocrystals. Physical Sciences Reviews, 2018, 3, .	0.8	2
66	Cyclic Penta-Twinned Rhodium Nanobranches as Superior Catalysts for Ethanol Electro-oxidation. Journal of the American Chemical Society, 2018, 140, 11232-11240.	6.6	133
67	Morphology led high dispersion of Pt icosahedral nanocrystals on carbon nanotubes for enhanced electro-catalytic activity and stability. Chemical Communications, 2018, 54, 10855-10858.	2.2	6
68	Facile Synthesis of Pd@Pt3- 4L Core-Shell Octahedra with a Clean Surface and Thus Enhanced Activity toward Oxygen Reduction. ChemCatChem, 2017, 9, 376-376.	1.8	0
69	Electrocatalysis of Ethylene Glycol Oxidation on Bare and Bi-Modified Pd Concave Nanocubes in Alkaline Solution: An Interfacial Infrared Spectroscopic Investigation. ACS Catalysis, 2017, 7, 2033-2041.	5.5	77
70	Platinum-nickel alloy excavated nano-multipods with hexagonal close-packed structure and superior activity towards hydrogen evolution reaction. Nature Communications, 2017, 8, 15131.	5.8	364
71	The synergy between atomically dispersed Pd and cerium oxide for enhanced catalytic properties. Nanoscale, 2017, 9, 6643-6648.	2.8	63
72	Selective Catalytic Performances of Noble Metal Nanoparticle@MOF Composites: The Concomitant Effect of Aperture Size and Structural Flexibility of MOF Matrices. Chemistry - A European Journal, 2017, 23, 11397-11403.	1.7	50

#	Article	IF	CITATIONS
73	Tunable magnetic pole inversion in multiferroic BiFeO <sub>3</sub> –DyFeO <sub>3</sub> solid solution. Journal of Materials Chemistry C, 2017, 5, 4063-4067.	2.7	12
74	Facile Synthesis of Pd@Pt <sub>3<b>–</b>4L</sub> Core–Shell Octahedra with a Clean Surface and Thus Enhanced Activity toward Oxygen Reduction. ChemCatChem, 2017, 9, 414-419.	1.8	18
75	Ternary Alloys Encapsulated within Different MOFs via a Selfâ€Sacrificing Template Process: A Potential Platform for the Investigation of Sizeâ€Selective Catalytic Performances. Small, 2017, 13, 1700683.	5.2	31
76	Excavated octahedral Pt-Co alloy nanocrystals built with ultrathin nanosheets as superior multifunctional electrocatalysts for energy conversion applications. Nano Energy, 2017, 39, 582-589.	8.2	130
77	Synthesis and enhanced electromagnetic wave absorption performance of amorphous CoxFe10-x alloys. Journal of Alloys and Compounds, 2017, 726, 1255-1261.	2.8	35
78	Synthesis of single-crystal hyperbranched rhodium nanoplates with remarkable catalytic properties. Science China Materials, 2017, 60, 685-696.	3.5	18
79	Excavated Cubic Platinum–Tin Alloy Nanocrystals Constructed from Ultrathin Nanosheets with Enhanced Electrocatalytic Activity. Angewandte Chemie, 2016, 128, 9167-9171.	1.6	20
80	A Phytic Acid Induced Superâ€Amphiphilic Multifunctional 3D Grapheneâ€Based Foam. Angewandte Chemie - International Edition, 2016, 55, 3936-3941.	7.2	176
81	Excavated Cubic Platinum–Tin Alloy Nanocrystals Constructed from Ultrathin Nanosheets with Enhanced Electrocatalytic Activity. Angewandte Chemie - International Edition, 2016, 55, 9021-9025.	7.2	111
82	Well-faceted noble-metal nanocrystals with nonconvex polyhedral shapes. Chemical Society Reviews, 2016, 45, 3207-3220.	18.7	111
83	A comparative investigation of electrocatalysis at Pt monolayers on shape-controlled Au nanocrystals: facet effect versus strain effect. Journal of Materials Chemistry A, 2016, 4, 15845-15850.	5.2	19
84	Facile Synthesis of Pt–Pd Alloy Nanocages and Pt Nanorings by Templating with Pd Nanoplates. ChemNanoMat, 2016, 2, 1086-1091.	1.5	16
85	Engineering high-energy surfaces of noble metal nanocrystals with enhanced catalytic performances. Nano Today, 2016, 11, 661-677.	6.2	76
86	Shape-controlled synthesis of CO-free Pd nanocrystals with the use of formic acid as a reducing agent. Chemical Communications, 2016, 52, 12594-12597.	2.2	17
87	Efficiently Enhancing Visible Light Photocatalytic Activity of Faceted TiO <sub>2</sub> Nanocrystals by Synergistic Effects of Core–Shell Structured Au@CdS Nanoparticles and Their Selective Deposition. ACS Applied Materials & Interfaces, 2016, 8, 21326-21333.	4.0	43
88	Controlled Encapsulation of Flower-like Rh–Ni Alloys with MOFs via Tunable Template Dealloying for Enhanced Selective Hydrogenation of Alkyne. ACS Applied Materials & Interfaces, 2016, 8, 31059-31066.	4.0	52
89	Probing the structural flexibility of MOFs by constructing metal oxide@MOF-based heterostructures for size-selective photoelectrochemical response. Nanoscale, 2016, 8, 13181-13185.	2.8	27
90	Templated synthesis of diluted magnetic semiconductors using transition metal ion-doped metal–organic frameworks: the case of Co-doped ZnO. CrystEngComm, 2016, 18, 4121-4126.	1.3	26

#	Article	IF	CITATIONS
91	Ag@Au Concave Cuboctahedra: A Unique Probe for Monitoring Au-Catalyzed Reduction and Oxidation Reactions by Surface-Enhanced Raman Spectroscopy. ACS Nano, 2016, 10, 2607-2616.	7.3	125
92	Pt-Based Icosahedral Nanocages: Using a Combination of {111} Facets, Twin Defects, and Ultrathin Walls to Greatly Enhance Their Activity toward Oxygen Reduction. Nano Letters, 2016, 16, 1467-1471.	4.5	228
93	Efficiently enhancing the photocatalytic activity of faceted TiO <sub>2</sub> nanocrystals by selectively loading α-Fe <sub>2</sub> O <sub>3</sub> and Pt co-catalysts. RSC Advances, 2016, 6, 29794-29801.	1.7	22
94	A facile surfactant-free synthesis of Rh flower-like nanostructures constructed from ultrathin nanosheets and their enhanced catalytic properties. Nano Research, 2016, 9, 849-856.	5.8	56
95	Size controllable redispersion of sintered Au nanoparticles by using iodohydrocarbon and its implications. Chemical Science, 2016, 7, 3181-3187.	3.7	46
96	Enhancing photo-reduction quantum efficiency using quasi-type II core/shell quantum dots. Chemical Science, 2016, 7, 4125-4133.	3.7	35
97	Ultrafast Photoinduced Interfacial Proton Coupled Electron Transfer from CdSe Quantum Dots to 4,4′-Bipyridine. Journal of the American Chemical Society, 2016, 138, 884-892.	6.6	52
98	Novel hydrogen storage properties of palladium nanocrystals activated by a pentagonal cyclic twinned structure. Nano Research, 2015, 8, 2698-2705.	5.8	33
99	Pd@Pt Core–Shell Concave Decahedra: A Class of Catalysts for the Oxygen Reduction Reaction with Enhanced Activity and Durability. Journal of the American Chemical Society, 2015, 137, 15036-15042.	6.6	296
100	Engineering a high energy surface of anatase TiO <sub>2</sub> crystals towards enhanced performance for energy conversion and environmental applications. RSC Advances, 2015, 5, 20396-20409.	1.7	79
101	Composition-tunable synthesis of Pt–Cu octahedral alloy nanocrystals from PtCu to PtCu3via underpotential-deposition-like process and their electro-catalytic properties. RSC Advances, 2015, 5, 18153-18158.	1.7	30
102	The effect of noble metal (Au, Pd and Pt) nanoparticles on the gas sensing performance of SnO <sub>2</sub> -based sensors: a case study on the {221} high-index faceted SnO <sub>2</sub> octahedra. CrystEngComm, 2015, 17, 6308-6313.	1.3	159
103	Platinum-based nanocages with subnanometer-thick walls and well-defined, controllable facets. Science, 2015, 349, 412-416.	6.0	854
104	A surfactant free synthesis and formation mechanism of hollow Cu <sub>2</sub> O nanocubes using Cl <sup>â^'</sup> ions as the morphology regulator. RSC Advances, 2015, 5, 61421-61425.	1.7	11
105	MOF-Derived Porous Co/C Nanocomposites with Excellent Electromagnetic Wave Absorption Properties. ACS Applied Materials & amp; Interfaces, 2015, 7, 13604-13611.	4.0	687
106	Palladium–platinum core-shell icosahedra with substantially enhanced activity and durability towards oxygen reduction. Nature Communications, 2015, 6, 7594.	5.8	440
107	Cu <sup>2+</sup> underpotential-deposition assisted synthesis of Au and Au–Pd alloy nanocrystals with systematic shape evolution. CrystEngComm, 2015, 17, 5556-5561.	1.3	16
108	Synthesis of composition-tunable octahedral Pt–Cu alloy nanocrystals by controlling reduction kinetics of metal precursors. Science Bulletin, 2015, 60, 1002-1008.	4.3	26

#	Article	IF	CITATIONS
109	Morphology evolution of NaTaO3 submicrometer single-crystals: from cubes to quasi-spheres. Science China Materials, 2015, 58, 281-288.	3.5	17
110	Synthesis of porous Cu <sub>2</sub> O/CuO cages using Cu-based metal–organic frameworks as templates and their gas-sensing properties. Journal of Materials Chemistry A, 2015, 3, 12796-12803.	5.2	341
111	Facile synthesis of (Ni,Co)@(Ni,Co) <sub>x</sub> Fe <sub>3â^'x</sub> O <sub>4</sub> core@shell chain structures and (Ni,Co)@(Ni,Co) <sub>x</sub> Fe <sub>3â^'x</sub> O <sub>4</sub> /graphene composites with enhanced microwave absorption. RSC Advances, 2015, 5, 70849-70855.	1.7	21
112	Pd–Cu Bimetallic Tripods: A Mechanistic Understanding of the Synthesis and Their Enhanced Electrocatalytic Activity for Formic Acid Oxidation. Advanced Functional Materials, 2014, 24, 7520-7529.	7.8	134
113	A comparative study of crystallographic van der Waals radii. Zeitschrift Fur Kristallographie - Crystalline Materials, 2014, 229, 517-523.	0.4	35
114	Wet chemical synthesis of intermetallic Pt <sub>3</sub> Zn nanocrystals via weak reduction reaction together with UPD process and their excellent electrocatalytic performances. Nanoscale, 2014, 6, 7019-7024.	2.8	59
115	Unique Excavated Rhombic Dodecahedral PtCu <sub>3</sub> Alloy Nanocrystals Constructed with Ultrathin Nanosheets of High-Energy {110} Facets. Journal of the American Chemical Society, 2014, 136, 3748-3751.	6.6	226
116	Supersaturation-Controlled Shape Evolution of α-Fe <sub>2</sub> O <sub>3</sub> Nanocrystals and Their Facet-Dependent Catalytic and Sensing Properties. ACS Applied Materials & Interfaces, 2014, 6, 12505-12514.	4.0	196
117	High-Energy-Surface Engineered Metal Oxide Micro- and Nanocrystallites and Their Applications. Accounts of Chemical Research, 2014, 47, 308-318.	7.6	203
118	Understanding the Formation of Pentagonal Cyclic Twinned Crystal from the Solvent Dependent Assembly of Au Nanocrystals into Their Colloidal Crystals. Journal of Physical Chemistry Letters, 2013, 4, 3440-3444.	2.1	19
119	High-efficiently visible light-responsive photocatalysts: Ag3PO4 tetrahedral microcrystals with exposed {111} facets of high surface energy. Journal of Materials Chemistry A, 2013, 1, 12635.	5.2	100
120	Structure and multiferroic properties of Bi(1-x)DyxFe0.90Mg0.05Ti0.05O3 solid solution. Journal of Applied Physics, 2013, 113, .	1.1	13
121	Semiconductor@Metal–Organic Framework Core–Shell Heterostructures: A Case of ZnO@ZIF-8 Nanorods with Selective Photoelectrochemical Response. Journal of the American Chemical Society, 2013, 135, 1926-1933.	6.6	691
122	Controlled synthesis of concave Cu <sub>2</sub> 0 microcrystals enclosed by {hhl} high-index facets and enhanced catalytic activity. Journal of Materials Chemistry A, 2013, 1, 282-287.	5.2	98
123	Supersaturation-Dependent Surface Structure Evolution: From Ionic, Molecular to Metallic Micro/Nanocrystals. Journal of the American Chemical Society, 2013, 135, 9311-9314.	6.6	149
124	Surfactantâ€Concentrationâ€Dependent Shape Evolution of Au–Pd Alloy Nanocrystals from Rhombic Dodecahedron to Trisoctahedron and Hexoctahedron. Small, 2013, 9, 538-544.	5.2	88
125	Synthesis of Rhodium Concave Tetrahedrons by Collectively Manipulating the Reduction Kinetics, Facet-Selective Capping, and Surface Diffusion. Nano Letters, 2013, 13, 6262-6268.	4.5	66
126	Cu–Au alloy nanotubes with five-fold twinned structure and their application in surface-enhanced Raman scattering. Journal of Materials Chemistry, 2012, 22, 18192.	6.7	62

#	Article	IF	CITATIONS
127	Au–Cu alloy bridged synthesis and optoelectronic properties of Au@CuInSe <sub>2</sub> core–shell hybrid nanostructures. Journal of Materials Chemistry, 2012, 22, 1765-1769.	6.7	23
128	Carbonate ions-assisted syntheses of anatase TiO2 nanoparticles exposed with high energy (001) facets. RSC Advances, 2012, 2, 3251.	1.7	80
129	Synthesis and shape-dependent catalytic properties of CeO2 nanocubes and truncated octahedra. CrystEngComm, 2012, 14, 7579.	1.3	88
130	Synthesis and room temperature four-state memory prototype of Sr <sub>3</sub> Co <sub>2</sub> Fe <sub>24</sub> O <sub>41</sub> multiferroics. Applied Physics Letters, 2012, 101, 122903.	1.5	48
131	The preparation of spiral ZnO nanostructures by top-down wet-chemical etching and their related properties. Journal of Materials Chemistry, 2012, 22, 10924.	6.7	27
132	Synthesis of layered protonated titanate hierarchical microspheres with extremely large surface area for selective adsorption of organic dyes. CrystEngComm, 2012, 14, 7715.	1.3	42
133	Synthesis of spatially uniform metal alloys nanocrystals via a diffusion controlled growth strategy: The case of Au-Pd alloy trisoctahedral nanocrystals with tunable composition. Nano Research, 2012, 5, 618-629.	5.8	36
134	Palladium nanocrystals enclosed by {100} and {111} facets in controlled proportions and their catalytic activities for formic acid oxidation. Energy and Environmental Science, 2012, 5, 6352-6357.	15.6	358
135	Facile syntheses and enhanced electrocatalytic activities of Pt nanocrystals with {hkk} high-index surfaces. Nano Research, 2012, 5, 181-189.	5.8	92
136	Controlled Synthesis and Enhanced Catalytic and Gasâ€Sensing Properties of Tin Dioxide Nanoparticles with Exposed Highâ€Energy Facets. Chemistry - A European Journal, 2012, 18, 2283-2289.	1.7	103
137	Facile syntheses and electrocatalytic properties of porous Pd and its alloy nanospheres. Journal of Materials Chemistry, 2011, 21, 9620.	6.7	62
138	Fabrication of the SnO <sub>2</sub> /α-Fe <sub>2</sub> O <sub>3</sub> Hierarchical Heterostructure and Its Enhanced Photocatalytic Property. Journal of Physical Chemistry C, 2011, 115, 7874-7879.	1.5	88
139	Rational design and SERS properties of side-by-side, end-to-end and end-to-side assemblies of Au nanorods. Journal of Materials Chemistry, 2011, 21, 14448.	6.7	66
140	Intense and wavelength-tunable photoluminescence from surface functionalized MgO nanocrystal clusters. Journal of Materials Chemistry, 2011, 21, 7263.	6.7	36
141	Partially inverse spinel ZnFe2O4 with high saturation magnetization synthesized via a molten salt route. Applied Physics Letters, 2011, 99, .	1.5	34
142	Synthesis of Pdâ^'Pt Bimetallic Nanocrystals with a Concave Structure through a Bromide-Induced Galvanic Replacement Reaction. Journal of the American Chemical Society, 2011, 133, 6078-6089.	6.6	405
143	Synthesis of "Clean―and Well-Dispersive Pd Nanoparticles with Excellent Electrocatalytic Property on Graphene Oxide. Journal of the American Chemical Society, 2011, 133, 3693-3695.	6.6	857
144	Synthesis of Pd nanocrystals enclosed by {100} facets and with sizes <10 nm for application in CO oxidation. Nano Research, 2011, 4, 83-91.	5.8	436

#	Article	IF	CITATIONS
145	Synthesis and high electrocatalytic performance of hexagram shaped gold particles having an open surface structure with kinks. Nano Research, 2011, 4, 612-622.	5.8	50
146	Synthesis of Concave Palladium Nanocubes with Highâ€Index Surfaces and High Electrocatalytic Activities. Chemistry - A European Journal, 2011, 17, 9915-9919.	1.7	98
147	Scanning electrochemical microscopy development of instrumentation utilizing piezo-bimorph X-Y scanners. Chinese Journal of Chemistry, 2010, 13, 105-111.	2.6	1
148	A simple solvothermal route towards the morphological control of ZnO and tuning of its optical and photocatalytic properties. Science China Chemistry, 2010, 53, 1711-1717.	4.2	7
149	Syntheses and Properties of Micro/Nanostructured Crystallites with Highâ€Energy Surfaces. Advanced Functional Materials, 2010, 20, 3634-3645.	7.8	230
150	Room-temperature ferromagnetic/ferroelectric BiFeO3 synthesized by a self-catalyzed fast reaction process. Journal of Materials Chemistry, 2010, 20, 6512.	6.7	59
151	Synthesis of small silver nanocubes in a hydrophobic solvent by introducing oxidative etching with Fe(iii) species. Journal of Materials Chemistry, 2010, 20, 3586.	6.7	50
152	Synthesis of Tin Dioxide Octahedral Nanoparticles with Exposed Highâ€Energy {221} Facets and Enhanced Gasâ€Sensing Properties. Angewandte Chemie - International Edition, 2009, 48, 9180-9183.	7.2	405
153	Single-crystal-like hematite colloidal nanocrystal clusters: synthesis and applications in gas sensors, photocatalysis and water treatment. Journal of Materials Chemistry, 2009, 19, 6154.	6.7	139
154	Controlling Morphologies and Tuning the Related Properties of Nano/Microstructured ZnO Crystallites. Journal of Physical Chemistry C, 2009, 113, 584-589.	1.5	349
155	Versatile fabrication of aligned SnO <sub>2</sub> nanotube arrays by using various ZnO arrays as sacrificial templates. Journal of Materials Chemistry, 2009, 19, 1019-1023.	6.7	55
156	Substituent effect on the assembly of coordination polymers containing isophthalic acid and its derivatives. CrystEngComm, 2009, 11, 2548.	1.3	80
157	Polymorphic structures and properties of lead chromium phosphate Pb3Cr2(PO4)4. Journal of Materials Chemistry, 2009, 19, 6034.	6.7	3
158	Syntheses, crystal structures, and magnetic properties of three coordination polymers based on manganese(II) and 2,6-naphthalenedicarboxylate. Transition Metal Chemistry, 2008, 33, 1019-1026.	0.7	4
159	Epitaxial Growth of Heterogeneous Metal Nanocrystals: From Gold Nano-octahedra to Palladium and Silver Nanocubes. Journal of the American Chemical Society, 2008, 130, 6949-6951.	6.6	719
160	Twin-Crystal Nature of the Single-Crystal-Like Branched Cu <sub>2</sub> O Particles. Journal of Physical Chemistry C, 2008, 112, 13405-13409.	1.5	29
161	One-Step Preparation of Large-Scale Self-Assembled Monolayers of Cyanuric Acid and Melamine Supramolecular Species on Au(111) Surfaces. Journal of Physical Chemistry C, 2008, 112, 4209-4218.	1.5	86
162	Single Molecule Conductance of Dipyridines with Conjugated Ethene and Nonconjugated Ethane Bridging Group. Journal of Physical Chemistry C, 2008, 112, 3935-3940.	1.5	52

#	Article	IF	CITATIONS
163	Synthesis and characterization of a nickel metavanadate complex: Ni(pz)(V2O6) (pz = pyrazine). Journal of Coordination Chemistry, 2008, 61, 1575-1581.	0.8	3
164	Tip-enhanced Raman spectroscopy for investigating adsorbed species on a single-crystal surface using electrochemically prepared Au tips. Applied Physics Letters, 2007, 91, 101105.	1.5	87
165	One-step construction of ZnS/C and CdS/C one-dimensional core–shell nanostructures. Journal of Materials Chemistry, 2007, 17, 1326-1330.	6.7	23
166	The Origin of Green Emission of ZnO Microcrystallites:  Surface-Dependent Light Emission Studied by Cathodoluminescence. Journal of Physical Chemistry C, 2007, 111, 12091-12093.	1.5	62
167	In Situ STM Studies on the Underpotential Deposition of Antimony on Au(111) and Au(100) in a BMIBF4Ionic Liquid. Journal of Physical Chemistry C, 2007, 111, 10467-10477.	1.5	22
168	Formation of ZnO hexagonal micro-pyramids: a successful control of the exposed polar surfaces with the assistance of an ionic liquid. Chemical Communications, 2005, , 5572.	2.2	205
169	Growth of Silver Nanowires from Solutions:Â A Cyclic Penta-twinned-Crystal Growth Mechanism. Journal of Physical Chemistry B, 2005, 109, 9416-9421.	1.2	135
170	Tailoring the Optical Property by a Three-Dimensional Epitaxial Heterostructure:Â A Case of ZnO/SnO2. Journal of the American Chemical Society, 2005, 127, 11777-11784.	6.6	195
171	Spontaneous transformation of selenium from monoclinic micro-balls to trigonal nano-rods in ethanol solution. Journal of Materials Chemistry, 2003, 13, 1447.	6.7	14
172	Influence of reconstruction on the structure of self-assembled normal-alkane monolayers on Au(111) surfaces. Physical Chemistry Chemical Physics, 2002, 4, 1486-1489.	1.3	16
173	Ag clusters electrochemically reduced in stearic acid Langmuir-Blodgett films and their structural characterizations. Science in China Series B: Chemistry, 1997, 40, 397-404.	0.8	3
174	Improvement of silicon etching resolution using the confined etchant layer technique. Science Bulletin, 1997, 42, 1318-1319.	1.7	5